Terrain-Constrained A* Algorithm for Autonomous Navigation of Tracked Vehicles in High-Relief Off-Road Terrains

V. H. Mullainathan
Department of Robotics and Automation Engineering
PSG College of Technology
Coimbatore, India
mullai2004@gmail.com

T. N. Sivatmiga
Department of Robotics and Automation Engineering
PSG College of Technology
Coimbatore, India
sivatmiga@gmail.com

Author Name
Affiliation
author@email.com

Abstract* - This paper presents a terrain-aware path planning framework for autonomous navigation in unstructured, high-relief environments using an enhanced A* algorithm. The classical A* algorithm, while effective in structured grids, fails to accommodate real-world terrain constraints such as slope and elevation variability. This work addresses these limitations through a Terrain-Constrained A* variant that incorporates elevation and slope masks derived from high-resolution Digital Elevation Models (DEMs) and terrain slope rasters. The algorithm supports subpixel search, 32-directional angular movement, and slope constraint filtering, improving path feasibility for heavy tracked vehicles. A GUI was developed using PyQt5 for terrain data interaction, path visualization, and export. The system was evaluated over five terrain scenarios in the Western Himalayas using SRTM DEMs, with three algorithm variants benchmarked for slope compliance, elevation gain, and path smoothness. Results show that the Terrain-Constrained A* consistently ensures 100% slope compliance while producing navigable paths suited for tactical vehicle deployment in high-altitude, infrastructure-deficient environments.

***Index Terms* - A* algorithm, autonomous navigation, digital elevation model, slope filtering, terrain-aware planning, tracked vehicles**

I. Introduction

Autonomous navigation in unstructured environments such as mountainous terrains, glacial regions, and undeveloped landscapes has emerged as a critical capability in defence logistics, remote exploration, and disaster response. These regions typically lack structured road infrastructure, exhibit irregular elevation profiles, and often present hazardous surface conditions that make manual navigation difficult and error-prone. In such scenarios, autonomous systems—particularly tracked or wheeled ground vehicles—must rely heavily on terrain-aware path planning to ensure safety, mobility, and operational effectiveness.

Traditional path planning algorithms like A* are well-suited for structured, grid-based environments. However, when applied directly to Digital Elevation Models (DEMs)—which are essentially 2D raster grids encoding terrain elevation—they exhibit limitations. These include generation of jagged, zigzag paths due to movement being restricted to discrete grid directions (4, 8, or n-way connectivity), lack of awareness of terrain difficulty such as slope, and excessive proximity to obstacles. This phenomenon, often referred to as **"obstacle hugging"**, arises from a poorly constructed cost-map that fails to penalize traversals near hazardous regions. Without integrating terrain semantics into the cost function, the planner may propose paths that are mathematically optimal in terms of distance but physically infeasible for the vehicle.

To address these shortcomings, it is necessary to build a geospatially informed base map composed of multiple terrain layers derived from remote sensing data. These include:

- Digital Elevation Model (DEM): Captures elevation values, enabling computation of slope and elevation gain/loss.
- Slope Raster: Quantifies terrain steepness, derived from DEM using terrain gradient analysis.
- GO/NO-GO Mask: A binary layer identifying traversable and non-traversable areas based on predefined thresholds of slope and elevation.

The accuracy and fidelity of these base layers directly impact the path planning outcome. A coarse or noisy slope map, for example, may result in paths being routed through steep or unstable terrain. Conversely, a well-defined cost

surface—built from precisely filtered and resampled terrain data—ensures that the planner avoids such regions and adheres to vehicle-specific constraints (e.g., maximum allowable slope for tracked tankers is ±35°).

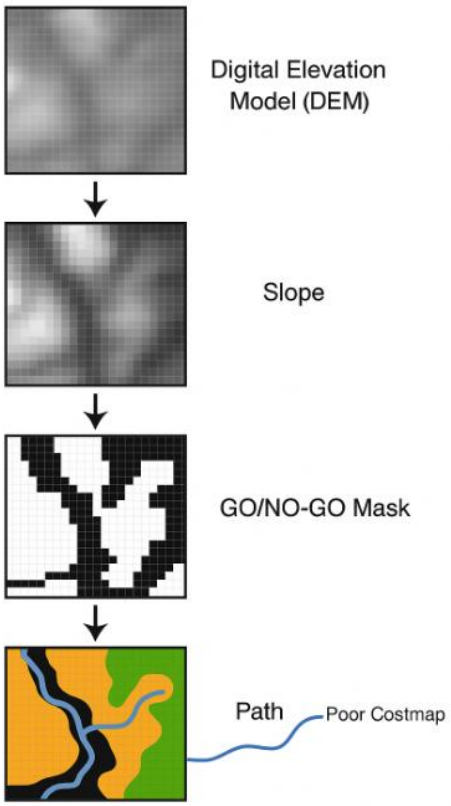

Fig 1. Base layer construction and its impact on terrain-aware path planning.

The Figure 1 shows how DEM, slope, and GO/NO-GO masks form the base map for path planning. Accurate layers help avoid unsafe terrain, while poor cost-maps lead to obstacle hugging and unrealistic paths.

This study proposes an enhanced A* algorithm that incorporates terrain masking, high-resolution subpixel movement, and 32-directional angular search. The goal is to achieve safe, smooth, and realistic path trajectories that respect the physical limits of off-road autonomous vehicles operating in complex natural terrains.

II. Related Work

Path planning in unstructured or off-road environments has been a subject of intensive research, particularly in applications involving planetary exploration, defence logistics, and disaster-response robotics. While the A* algorithm remains a classical choice for graph-based search due to its optimality and deterministic behaviour, its direct application to terrain data such as Digital Elevation Models (DEMs) leads to several limitations. These include grid-induced zigzag artifacts, poor handling of elevation gain, and lack of slope or terrain compliance.

*A. Limitations of Classical A**

Standard implementations of A* use 4- or 8-directional movement on raster grids, resulting in staircase-like paths that are unsuitable for wheeled or tracked vehicles. Furthermore, cost calculations typically do not account for terrain gradient, leading to infeasible paths in hilly or mountainous environments. For example, paths that follow steep slopes or tightly hug obstacles may be mathematically optimal in 2D but are physically unrealistic for ground vehicle traversal.

B. Terrain-Integrated A Variants*

To address these challenges, numerous improvements have been proposed:

Slope-aware A*: Hong et al. [1] introduced terrain slope as a cost multiplier in the A* cost function, significantly improving path feasibility. Their method also implemented bidirectional search to reduce computation time by narrowing the search domain.

Theta*: This any-angle A* variant proposed by Nash et al. [3] relaxes grid adjacency constraints by using line-of-sight checks, enabling smoother and more direct paths across DEMs. It avoids the typical jaggedness of classical A*.

Angle-Constrained A*: Yakovlev and Andreychuk [4] developed the LIAN algorithm, enforcing angular continuity between nodes, which reduces sharp turns and improves manoeuvrability for UAVs and ground robots.

C. Hybrid Approaches and Two-Stage Planning

PRM + A*: Zheng et al. [2] introduced a two-stage planning strategy where Probabilistic Roadmaps (PRMs) are used to generate an initial coarse path, later refined by A*. Morphological dilation is applied to define a narrowed search space for the A* phase, significantly reducing computational cost.

Hybrid A*: Hartzell [7] integrated vehicle kinematic constraints into the A* framework, resulting in trajectories that align better with turning radii and motion models. While computationally intensive, it demonstrated better adherence to vehicle dynamics in semi-structured terrain.

TABLE 1. COMPARISON OF A* VARIANTS FOR TERRAIN-AWARE PATH PLANNING

Variant	Enhancement	Terrain Integration	Advantages	Limitations
Classical A*	4-/8-direction grid search	None	Simple, fast, deterministic	zigzag paths; obstacle hugging
Theta* [3]	Any-angle path via line-of-sight	Optional elevation context	Smooth, direct paths	Assumes perfect line-of-sight; lacks terrain masking
Hybrid A* [7]	Vehicle motion model + A* logic	Map + Kinematics constraints	Generates kinematically feasible paths	Higher computational cost; vehicle-specific

Angle-Constrained A* [4]	Enforces angular continuity	Grid map with angle constraints	Smooth transitions; good for wheeled vehicles	Not optimal in presence of sharp elevation changes
PRM + A* [2]	Two-stage: PRM + refined A* with dilation	DEM + Slope + Dilated cost-map	Fast coarse planning + accurate fine planning	Requires pre-processing; not reactive
Energy-Aware A* [6]	Composite metric using energy and terrain slope	DEM + terrain energy model	Optimizes energy use along path	Limited terrain model detail; lacks slope enforcement
Terrain-Constrained A* (This Work)	Slope-masked search + subpixel + 32-dir A*	DEM + Slope + GO/NO-GO Mask	100% slope compliance; smooth paths; terrain safety ensured	Slower; assumes static terrain; no kinematic constraints yet

Table 1 provides a comparison of various A path planning algorithms and their adaptations for terrain-aware navigation. While classical A* is computationally efficient, it lacks slope and elevation awareness. Variants like slope-aware A*, Theta*, and Hybrid A* offer improvements in path realism and terrain safety. The proposed Terrain-Constrained A* in this work uniquely combines slope masking, subpixel movement, and high-directionality for physically feasible navigation in unstructured terrains.*

D. Terrain Modeling and GIS Support

Cost-Map Precision: Wu et al. [5] showed that combining terrain roughness, obstacle height, and slope in a traversability map enables planetary rovers to plan safer paths. Similarly, Saad et al. [6] proposed an energy-efficient routing method that weighs terrain slope against energy consumption, although it lacked real-time adaptability.

GIS-based Terrain Feasibility: Kumar et al. [10] highlighted the role of Geographic Information Systems (GIS) in generating detailed terrain overlays including slope, elevation, and hydrology. These layers, when fused into a cost-map, significantly improve planner awareness of terrain constraints.

SLAM for Localization: ORB-SLAM3 [9] is often used in conjunction with terrain-aware planning, offering robust visual and inertial localization in GPS-denied areas. Though not a planner itself, its output enables more reliable terrain referencing in real-time.

E. Research Gaps

Despite notable advancements in terrain-aware path planning, several limitations persist in current approaches. Most existing methods emphasize heuristic optimization or directional refinement but do not incorporate strict slope enforcement, which is critical for ensuring physical feasibility in off-road navigation. Additionally, the construction of cost-maps is often empirical and lacks rigorous filtering, leading to issues such as obstacle hugging or the generation of unrealistic routes through hazardous terrain. Furthermore, many terrain-constrained planning methods remain computationally intensive, posing challenges for real-time deployment in mission-critical applications where responsiveness is essential.

This paper addresses these gaps by proposing a terrain-constrained A* planner that combines high-resolution DEM filtering, slope-based GO/NO-GO masking, subpixel search, and GUI-based interaction. The approach ensures 100% slope compliance while maintaining path feasibility across high-relief terrain.

III. Study Area and Data Set

A. Study Region

The region selected for this study lies in the Western Himalayan sector of northern India, characterized by steep elevation gradients, glacial valleys, and minimal anthropogenic infrastructure. This terrain is highly representative of real-world off-road operational zones such as military forward areas, high-altitude supply routes, and disaster-struck or unmapped regions. Such areas pose significant challenges for autonomous navigation due to sharp terrain transitions, sparse landmark features, and the absence of road network connectivity. Therefore, any autonomous vehicle navigating these regions must rely entirely on terrain-informed planning derived from remote sensing data.

B. Terrain Characteristics

The topography of the study area is defined by elevation ranges spanning from approximately 2700 meters to 5000 meters, with slopes frequently exceeding 30 degrees, especially along valleys and ridgelines. The terrain features a mix of surface types, including scree, snow patches, and loose gravel, all of which impact the stability and traversability of ground vehicles. These conditions make traditional A* path planning highly susceptible to failure, often producing paths that are impractical or unsafe unless terrain constraints are explicitly enforced during the planning process.

C. Data Sources and Preprocessing

Table 2. Terrain Data Layers Used for Path Planning and Their Functional Roles

Layer	Source	Resolution	Purpose
DEM	USGS/SRTMGL1_003 via GEE	30 meters	Base elevation model
Slope Raster	Derived from DEM using *ee.Terrain.slope()*	30 meters	To calculate terrain steepness
GO/NO-GO Mask	Binary mask based on slope ≤ 35°	30 meters	Defines admissible search space for A*

To accurately model the terrain for autonomous path planning, multiple raster-based datasets were utilized.

These included a Digital Elevation Model (DEM), a derived slope raster, and a binary GO/NO-GO mask. The details of each layer are summarized in Table 2.

All data was accessed and processed using Google Earth Engine (GEE), a cloud-based geospatial analysis platform. Raster preprocessing involved several key steps to ensure consistency and usability. The region of interest was first clipped from the global dataset, followed by resampling all raster layers to a consistent spatial resolution of 30 meters. These processed layers were then exported in GeoTIFF format for integration with the local Python-based path planning environment.

D. Importance of Data Layer Accuracy

The quality and reliability of the input raster datasets have a direct and significant impact on the effectiveness of the path planning algorithm. The spatial granularity of the DEM affects how accurately terrain gradients are captured; a lower-resolution DEM may smooth over critical features such as cliffs or ridgelines, resulting in inaccurate slope estimates. The slope rasters, derived from DEMs, must be spatially aligned and consistently scaled to avoid false classifications of traversable or non-traversable zones. Most importantly, the construction of the cost-map particularly the GO/NO-GO mask—plays a pivotal role in guiding the planner through safe terrain. An imprecise or noisy cost-map can lead to poor route decisions, such as hugging steep terrain edges or descending into unstable regions. On the other hand, a well-filtered and terrain-compliant cost-map ensures that the planner respects terrain limitations and produces paths suitable for tracked vehicle deployment in high-relief environments.

IV. Path Planning Algorithm

A. Overview of A in Terrain Context*

The A* algorithm is a graph-based pathfinding method that computes an optimal route between two points by minimizing a cost function defined as $f(n) = g(n) + h(n)$ represents the actual cost from the start node to the current node and $h(n)$ denotes a heuristic estimate of the remaining cost to reach the goal. While A* performs well in structured grid environments, its direct application to terrain datasets such as DEMs poses several challenges. These elevation rasters, though spatially accurate, are treated as discrete 2D grids, leading to coarse and unrealistic paths that may traverse steep or untraversable regions. Furthermore, without accounting for slope or physical constraints, traditional A* may produce optimal but infeasible solutions, particularly in high-relief environments.

To overcome these challenges, the A* algorithm was enhanced with slope filtering, terrain masking, subpixel search resolution, and a high-directionality movement model. These modifications ensure that the planner not only seeks the shortest path but also one that is physically navigable by ground vehicles operating in rugged terrains.

B. A Variants Implemented*

Three progressively refined variants of the A* algorithm were developed to investigate the impact of terrain constraints and path resolution. The first variant, termed Simple A*, operates over the DEM using standard 8-directional grid movement and assumes all terrain is equally traversable. This basic model does not incorporate any slope or elevation filtering and often produces jagged, unrealistic routes.

The second variant, Resampling A*, improves upon the basic model by introducing subpixel resolution, allowing interpolated movement between grid cells. This yields visually smoother paths that better approximate continuous terrain traversal. However, it still lacks awareness of terrain difficulty and does not enforce slope constraints.

The third and most advanced variant, Terrain-Constrained A*, integrates multiple enhancements including a GO/NO-GO mask based on slope filtering, 32-directional angular movement for higher spatial resolution, and subpixel discretization for refined path generation. This implementation strictly avoids terrain violating predefined slope limits, ensuring that the planned route is both smooth and safe for tracked vehicles.

C. Movement Model and Resolution

The choice of movement model significantly influences the realism of the computed path. Simple A* limits motion to cardinal and inter-cardinal directions (up to 8), leading to abrupt direction changes and artificial staircasing in the route. In contrast, the Terrain-Constrained A* variant employs a 32-directional angular movement model that allows finer directional control. By discretizing the angular space and interpolating movement vectors, this model facilitates natural transitions along terrain contours, reducing path artifacts and improving navigability. Additionally, subpixel resolution further smooths the path by allowing intermediate steps within each raster cell, effectively increasing the planner's sensitivity to terrain features.

D. Terrain Constraint Enforcement

To ensure that the planner avoids unsafe regions, terrain constraint enforcement is applied as a preprocessing step. A GO/NO-GO binary mask is created using the slope raster, where each cell is classified as traversable or non-traversable based on a defined threshold—typically 35°, representing the operational slope limit for heavy tracked vehicles. Optionally, elevation bounds can also be applied to exclude terrain that lies outside vehicle operational limits. This binary mask is then used to constrain the A* search, allowing expansion only within the defined safe region. The result is a significant reduction in both search space and false feasibility, with guaranteed compliance to slope constraints.

E. Cost and Heuristic Functions

The planner uses Euclidean distance to compute the actual movement cost *g(n)* between adjacent nodes, which supports diagonal and non-orthogonal movement required for realistic off-road navigation. The heuristic function *h(n)* is also Euclidean, ensuring admissibility and preserving the optimality guarantees of A*. In this implementation, slope values are not used as soft penalties in the cost function but instead serve as hard constraints enforced through terrain masking. This strict filtering guarantees that no portion of the path traverses terrain exceeding the permissible slope, improving both safety and path reliability.

F. GUI Integration and Path Output

To support user interaction and terrain inspection, a graphical user interface (GUI) was developed using PyQt5 and integrated with raster handling libraries. Users can load DEM and slope rasters, define planning constraints such as slope thresholds and elevation limits, and interactively select start and goal positions on the terrain map. Once computed, the planned path is visualized directly on the DEM, color-coded by slope segments to highlight varying terrain difficulty. The GUI also generates elevation profile plots, visited node maps, and path overlays, which are saved in image and CSV formats. This interface facilitates both debugging and deployment, making the system accessible for practical off-road mission planning.

V. Experiment and Results

A. Experimental Setup

To assess the performance of the proposed terrain-aware A* path planning variants, a series of experiments were conducted using high-resolution topographic data from the Western Himalayas. This region was chosen due to its complex and varied terrain features, including steep gradients, deep valleys, and rugged ridgelines, making it a suitable testbed for evaluating off-road navigation algorithms. A consistent set of input layers—comprising a 30-meter resolution Digital Elevation Model (DEM) and the corresponding slope raster—was used across all experiments to maintain uniformity in evaluation.

The implementation was developed in Python 3.11, utilizing libraries such as NumPy, Rasterio, GDAL, and PyQt5 for terrain processing, algorithm execution, and visualization. All experiments were run on a system with an Intel Core i5-11400H processor, 16 GB of RAM, and Windows 11. Five test cases were designed by selecting different start and goal locations over the terrain. Each test was executed independently using the three algorithm variants—Simple A*, Resampling A*, and Terrain-Constrained A*—enabling direct comparison of their computational performance and terrain adaptability under identical conditions.

B. Evaluation Metrics

The performance of each path planning variant was evaluated using both computational and terrain-based metrics. These include:

- **Computation Time (s):** The total time taken by the algorithm to generate a valid path.
- **Path Length (m):** The total Euclidean distance of the computed path.
- **Elevation Gain (m):** The sum of all positive elevation changes along the path.
- **Average Slope (°):** Mean slope encountered along the traversable path segments.
- **Maximum Slope (°):** The steepest slope value encountered along the path.
- **Slope Violations (>35°):** Number of path segments exceeding the safe slope threshold.
- **Slope Compliance (%):** Proportion of the path that remains within slope limits.

These metrics provide a comprehensive assessment of the path's feasibility, efficiency, and adherence to physical constraints of tracked vehicle navigation.

C. Test Case Results

Across all five test cases, the Terrain-Constrained A* consistently demonstrated superior compliance with slope constraints. It maintained 100% slope compliance by strictly avoiding regions with slope values exceeding 35°, although at the cost of increased computation time.

The Simple A* variant was computationally the fastest but frequently traversed steep and unrealistic terrain. The Resampling A* offered smoother paths and better slope statistics than Simple A*, but still resulted in multiple slope violations due to the lack of masking.

TABLE 3. SUMMARY OF EVALUATION METRICS CASE-1

Variant	Time (s)	Length (m)	Elev. Gain (m)	Avg. Slope (°)	Max Slope (°)	Violations	Compliance (%)
Simple A*	0.08	3309.97	491	22.61	58	48	57.89
Resampling A*	0.91	3811.08	542	20.38	43	17	89.44
Terrain-Constrained A*	950.86	3732.81	483	18.29	35	0	100.00

The results presented in Table 3 correspond to a test case where the start and goal positions were located at pixel coordinates (161, 266) and (201, 153), respectively. This pattern of results held across all scenarios. Terrain-Constrained A* always produced paths that were physically feasible, even in highly rugged areas, making it the most suitable for real-world deployment.

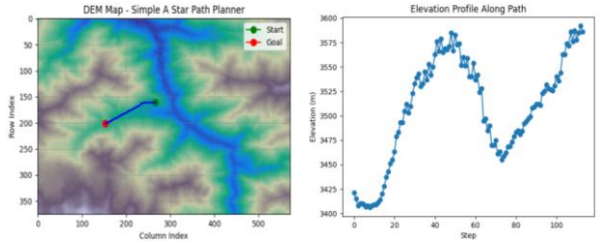

Fig 2. Simple a* path output – DEM overlay and elevation profile

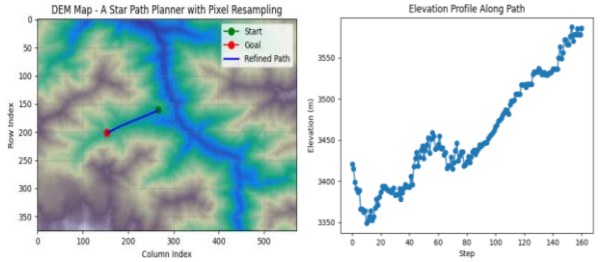

Fig 3. Resampling A* Path Output – DEM overlay and Elevation Profile

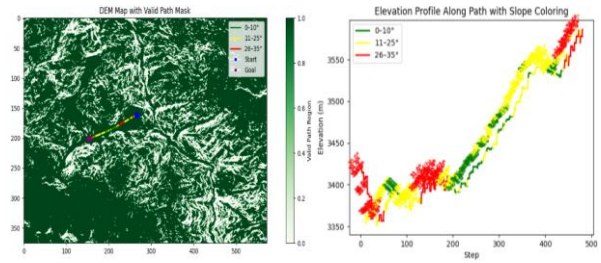

Fig 4. Terrain-Constrained A* Path on Valid Mask and Elevation Profile with Slope Colouring

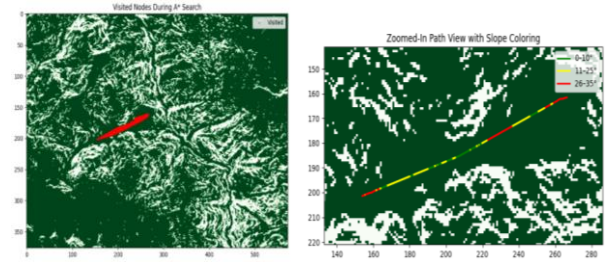

Fig 5. Terrain-Constrained A* Visited Nodes Map and Zoomed-In Path Segment

TABLE 4. SUMMARY OF EVALUATION METRICS CASE-2

Variant	Time (s)	Length (m)	Elev. Gain (m)	Avg. Slope (°)	Max Slope (°)	Violations	Compliance (%)
Simple A*	0.07	3215.14	586	27.51	58	41	57.29
Resampling A*	0.95	3481.31	708	29.23	55	61	57.93
Terrain-Constrained A*	2901.24	3981.39	631	27.96	35	0	100

The results presented in Table 4 correspond to a test case where the start and goal positions were located at pixel coordinates (72, 163) and (167, 120), respectively.

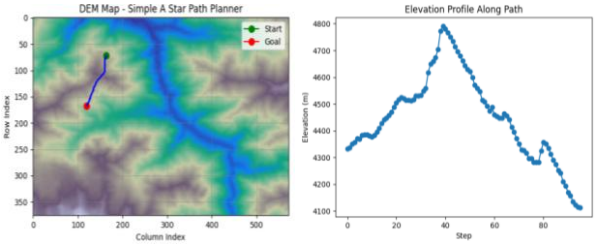

Fig 6. Simple A* Path Output – DEM overlay and Elevation Profile

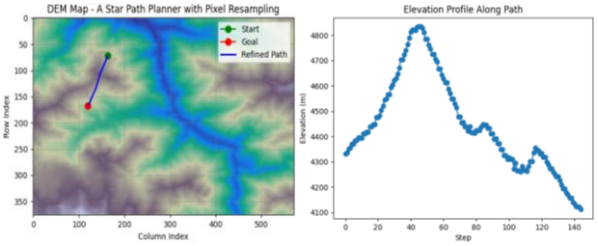

Fig 7. Resampling A* Path Output – DEM overlay and Elevation Profile

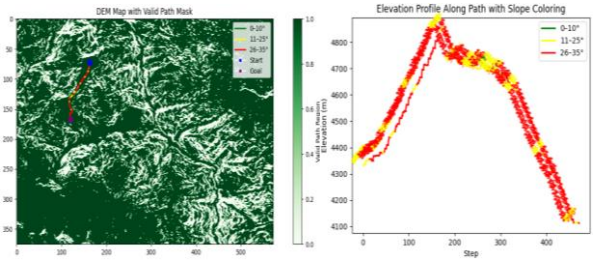

Fig 8. Terrain-Constrained A* Path on Valid Mask and Elevation Profile with Slope Colouring

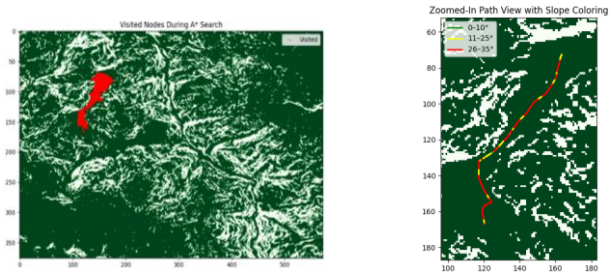

Fig 9. Terrain-Constrained A* Visited Nodes Map and Zoomed-In Path Segment

D. Visual Diagnostics

For both Case 1 and Case 2, visual diagnostics were generated to qualitatively assess how each A* variant responded to terrain features such as ridgelines, valleys, and steep slopes. These visuals provided critical insights into the planner's ability to navigate high-relief landscapes.

In Case 1, the path overlay clearly shows that the Simple A* algorithm cut across steep gradients, violating slope constraints and resulting in a jagged path with several abrupt turns. The Resampling A* variant offered smoother trajectories but still intruded into regions with slopes exceeding 35°, especially near the midsection of the path. The Terrain-Constrained A*, in contrast, followed the natural contour of the terrain, maintaining consistent offset from steep regions and adhering strictly to the GO/NO-GO mask. The elevation profile for this case confirmed a

gradual ascent with minimal elevation spikes, while the visited node map showed a highly focused and slope-compliant search space for the Terrain-Constrained variant, unlike the wide, unconstrained expansions seen in the other two methods.

In **Case 2**, similar patterns were observed but with more pronounced differences in performance. The Simple A* again produced a direct but infeasible path across a steep valley, with the elevation profile showing sharp altitude transitions. Resampling A* demonstrated even more slope violations than in Case 1, suggesting its limitations in steeper terrain sections. The Terrain-Constrained A* successfully avoided all unsafe zones, even if it meant increasing path length and computational time. Its visited node map showed controlled expansion strictly within the valid slope range, and the zoomed terrain view illustrated how it rerouted around a high-slope ridge that the other variants crossed unsafely.

Together, these visual outputs path overlays, elevation plots, visited node expansions, and zoomed terrain interactions validated the operational benefits of incorporating terrain filtering and high-resolution directional search into the A* planning framework.

E. Comparative Insights

The comparative analysis of Case 1 and Case 2 reinforces the consistent superiority of the Terrain-Constrained A* variant in generating physically feasible and terrain-compliant paths. By incorporating slope masks and restricting expansion to valid terrain, it effectively eliminated slope violations across both test cases. The use of 32-directional angular movement, combined with subpixel resolution, allowed it to produce paths that aligned closely with natural terrain contours, significantly reducing unnatural zigzagging and sharp elevation transitions.

Although this variant incurred substantially higher computation times—particularly noticeable in Case 2—it delivered clear advantages in terms of route safety and suitability for tracked vehicles operating in rugged off-road conditions.

In contrast, Simple A* consistently underperformed due to its lack of terrain awareness. It frequently selected routes through steep terrain, resulting in multiple slope violations and poor compliance percentages. Resampling A* improved the smoothness of the path but demonstrated unpredictable behaviour in complex terrain, as evidenced by its higher number of violations in Case 2.

These results highlight the importance of incorporating explicit terrain constraints into the path planning process for deployment in real-world high-relief environments, where safety and operational feasibility.

Across all test cases, Terrain-Constrained A* demonstrated consistent slope adherence and feasibility, validating its suitability for high-relief operational deployment.

VI. Discussion

The comparative analysis conducted across multiple test cases highlights the operational trade-offs among the three A* variants and underscores the effectiveness of terrain-aware planning in unstructured, high-relief environments. The Terrain-Constrained A* consistently demonstrated 100% slope compliance, producing paths that not only adhered to physical terrain constraints but also exhibited smoother elevation transitions and more realistic trajectories compared to the other two variants.

One of the key findings is that integrating terrain semantics—specifically slope thresholds and elevation constraints—into the A* algorithm through precomputed GO/NO-GO masks significantly enhances path feasibility. Unlike methods that apply terrain influence as a soft cost penalty, hard masking ensures that no unsafe region is entered during the search process. This approach reduces the likelihood of paths hugging steep terrain boundaries or violating gradient limits, which is critical for vehicle stability in real-world deployment scenarios.

The computational cost of the Terrain-Constrained A* is notably higher, particularly in Test Case 2, where increased terrain complexity and higher angular resolution (32-directional movement) resulted in longer runtimes. However, this is a justifiable trade-off when safety and physical feasibility are prioritized over time efficiency. For military logistics, search and rescue missions, or any autonomous operation in sensitive terrain, this conservative planning approach is preferable.

The Simple A* variant, while computationally efficient, failed to produce usable paths in terrain with frequent slope violations. Its lack of elevation or gradient awareness renders it unsuitable for high-altitude or mountainous applications. Resampling A* addressed some of the spatial discretization issues by interpolating movements between pixels, resulting in visually smoother paths. However, without slope enforcement, it remained vulnerable to terrain hazards, particularly in steep valleys or ridges.

Furthermore, visual diagnostics such as elevation profiles and visited node maps reinforced the limitations of terrain-unaware methods. In contrast, Terrain-Constrained A* displayed focused search expansions and terrain-following path behaviour, clearly demonstrating its robustness.

The study also revealed the importance of high-resolution base layers. The quality of the DEM and slope raster directly affects the planner’s ability to discriminate between safe and unsafe terrain. Even minor artifacts or under-sampled slope features can introduce significant errors in unfiltered planners. Therefore, accurate preprocessing using tools like Google Earth Engine and

appropriate thresholding is essential for effective terrain masking.

In conclusion, the Terrain-Constrained A* algorithm, despite its higher computational cost, emerges as the most reliable solution for autonomous navigation in steep and rugged environments. Its integration of geospatial constraints, subpixel resolution, and multi-directional movement offers a viable path planning framework for real-world applications where terrain safety is paramount.

VII. Conclusion and Future Work

This study presented a terrain-aware enhancement of the classical A* algorithm for autonomous navigation in high-relief, off-road environments. By integrating geospatial terrain constraints—specifically slope-based GO/NO-GO masking—alongside subpixel resolution and 32-directional movement, the proposed Terrain-Constrained A* algorithm successfully addressed the limitations of traditional grid-based planners.

Experimental results across multiple test cases demonstrated that the Terrain-Constrained A* consistently achieved 100% slope compliance, producing physically feasible and smooth paths while navigating complex terrain features. While the method incurs higher computational overhead compared to simpler variants, the improvement in terrain adherence and vehicle safety justifies this trade-off for real-world applications such as military convoy planning, disaster response, and exploratory robotics in unstructured environments.

Future work will focus on optimizing the computation time of the Terrain-Constrained A* by incorporating hierarchical planning layers or GPU-accelerated expansion strategies. Additional research will explore dynamic replanning under real-time terrain changes using LiDAR or SLAM-based updates. Further, the current implementation can be extended to include vehicle kinematic models, such as turning radius and skid-steering dynamics, for even greater deployment realism. Integration with sensor data (e.g., soil type, water bodies, snow cover) and transition to a fully ROS 2-based navigation stack are also planned to support hardware-in-the-loop validation and field testing.

References

[1]. Z. Hong, Y. Xu, J. Yang, and Z. Tian, “Improved A-Star Algorithm for Long-Distance Off-Road Path Planning Using Terrain Data Map,” ISPRS International Journal of Geo-Information, vol. 10, no. 11, pp. 1–22, Nov. 2021.

[2]. X. Zheng, Z. Shen, D. Yang, and M. He, “Two-Stage Path Planning for Long-Distance Off-Road Path Planning Based on Terrain Data,” ISPRS International Journal of Geo-Information, vol. 13, no. 6, pp. 1–19, Jun. 2024.

[3]. D. Nash, K. Daniel, S. Koenig, and A. Felner, “Theta*: Any-Angle Path Planning on Grids,” Journal of Artificial Intelligence Research, vol. 39, pp. 533–579, 2010.

[4]. D. Yakovlev and A. Andreychuk, “Grid-Based Angle-Constrained Path Planning,” in Proc. European Conference on Mobile Robots (ECMR), 2015, pp. 1–6.

[5]. B. Wu, J. Liu, and Y. Li, “Terrain-Based Path Planning for Planetary Rovers Using Global and Local Maps,” Planetary and Space Science, vol. 187, pp. 1–10, 2020.

[6]. M. Saad, A. Al-Kaff, F. Garcia, and D. Martin, “Energy-Efficient Path Planning on Natural Terrains Using Terrain Slope Maps,” Applied Sciences, vol. 11, no. 15, pp. 1–20, 2021.

[7]. E. Hartzell, R. Siegwart, and M. Chli, “Hybrid A-Star Based Exploration Planner with Kinematic Constraints,” in Proc. IEEE International Conference on Robotics and Automation (ICRA), 2020, pp. 1532–1538.

[8]. T. Yairi et al., “Safe Planetary Rover Navigation by Terrain Evaluation Using Orbital Data and Machine Learning,” Acta Astronautica, vol. 186, pp. 318–331, 2021.

[9]. C. Campos, R. Elvira, J. J. Gómez Rodríguez, J. M. M. Montiel, and J. D. Tardós, “ORB-SLAM3: An Accurate Open-Source Library for Visual, Visual–Inertial, and Multi-Map SLAM,” IEEE Transactions on Robotics, vol. 37, no. 6, pp. 1874–1890, Dec. 2021.

[10]. A. Kumar, A. Singh, and R. Sharma, “Multi-Criteria Based Terrain Traversability Mapping for Off-Road Vehicles Using GIS,” Geomatics, Natural Hazards and Risk, vol. 13, no. 1, pp. 452–469, 2022.